SLAC-PUB-8163
July 1999

Direct Measurement of the Neutral Weak Dipole Moments of the τ Lepton*

The SLD Collaboration†
Stanford Linear Accelerator Center,
Stanford University, Stanford, CA 94309

Abstract

We present direct measurements of the neutral weak anomalous magnetic dipole moment, a_τ^w, and neutral weak electric dipole moment, d_τ^w, of the tau lepton. The dipole moments are measured by analyzing the decays of τ leptons produced in the annihilation of positrons and longitudinally polarized electrons on the Z boson resonance at the SLC. Using 6736 Z decays to $\tau^+\tau^-$ pairs selected from our 1993-1998 data sample we obtain $Re(a_\tau^w) = (0.26 \pm 1.24) \times 10^{-3}$, $Im(a_\tau^w) = (-0.02 \pm 0.66) \times 10^{-3}$, $Re(d_\tau^w) = (0.18 \pm 0.67) \times 10^{-17} e \cdot cm$, and $Im(d_\tau^w) = (-0.26 \pm 0.37) \times 10^{-17} e \cdot cm$.

Submitted to Physical Review Letters

*Work supported by Department of Energy contract DE–AC03–76SF00515 (SLAC).

A measurement of the neutral weak dipole moments of the tau lepton tests the standard model tenet that fundamental fermions are pointlike objects without structure. It also constitutes a general search for any new physics which couples more strongly to the third generation of fermions. Electroweak radiative corrections are expected to contribute $\Delta a_\tau^w \approx 2 \times 10^{-6}$ [1] and $\Delta d_\tau^w \approx 3 \times 10^{-37} e \cdot cm$ [2], where a_τ^w is the neutral weak anomalous magnetic dipole moment and d_τ^w is the neutral weak electric dipole moment. These values are extremely small compared to the sensitivity of present day experiments, so that a significant nonzero measurement of a_τ^w or d_τ^w would point to physics beyond the standard model. In particular, a significant nonzero measurement of d_τ^w would signal a new source of CP violation [3].

In this paper we directly measure a_τ^w and d_τ^w by analyzing the e^-, μ^-, π^-, and ρ^- decays of tau leptons produced in Z boson decay. The Z bosons are produced using longitudinally polarized electron beams. The most general $Z\tau^+\tau^-$ coupling can be written [4]

$$\Gamma^\mu_{Z\tau\tau} = i\frac{g}{2\cos\theta_W}\left[\gamma^\mu(g_V^\tau - g_A^\tau\gamma_5) + \frac{i}{2m_\tau}\sigma^{\mu\nu}q_\nu(\kappa - i\tilde{\kappa}\gamma_5)\right] \tag{1}$$

where q^ν is the Z momentum, θ_W is the weak mixing angle, g_V^τ and g_A^τ are the neutral weak vector and axial-vector coupling constants of the tau, m_τ is the tau mass, and $\sigma^{\mu\nu} = \frac{i}{2}[\gamma^\mu, \gamma^\nu]$. The neutral weak moments a_τ^w and d_τ^w are related to κ and $\tilde{\kappa}$ via

$$a_\tau^w = \frac{\kappa}{2\cos\theta_W\sin\theta_W}, \qquad d_\tau^w = \frac{e\tilde{\kappa}}{4\cos\theta_W\sin\theta_W m_\tau} \tag{2}$$

where e is the positron charge.

An anomalous neutral weak dipole moment enhances the transverse polarization of tau leptons. To illustrate this we examine the longitudinal and transverse tau polarizations [5] when $|\kappa|, |\tilde{\kappa}| \ll m_\tau/\sqrt{s} \ll 1$ and $g_V^\tau, g_V^e \to 0$:

$$\begin{aligned} T_x^\pm &= \frac{2\sqrt{s}}{m_\tau}\frac{\sin\Theta}{1+\cos^2\Theta}\left[-Re(\kappa)\cos\Theta \pm Im(\tilde{\kappa})P_e\right] \\ T_y^\pm &= \frac{2\sqrt{s}}{m_\tau}\frac{\sin\Theta}{1+\cos^2\Theta}\left[Im(\kappa)P_e \pm Re(\tilde{\kappa})\cos\Theta\right] \\ T_z^\pm &= \frac{2P_e\cos\Theta}{1+\cos^2\Theta} \end{aligned} \tag{3}$$

where $\sqrt{s}$ is the center-of-mass energy, Θ is the angle between the τ^- and initial e^-, and P_e is the longitudinal electron beam polarization, $-1 \leq P_e \leq 1$. The superscripts for $\mathbf{T}^{\pm}$ refer to the charge of the final state tau, while the subscripts x, y, z are defined such that the z-axis points in the direction of the τ^-, the x-axis is in the production plane, and the y-axis completes a right-handed orthogonal coordinate system.

Under the assumed conditions the longitudinal polarization, T_z, is insensitive to weak dipole moments, while the transverse polarizations, T_x and T_y, are directly proportional to the weak dipole moments. The contribution of the imaginary part of the weak dipole moment to the transverse tau polarization is linear in the longitudinal electron beam polarization. In fact, for large values of $|P_e|$ an experiment will be more sensitive to the imaginary parts than it will be to the real parts. In Eq.(3) we have suppressed terms proportional to $Im(\kappa)g_V^\tau \cos\Theta$ and $Im(\tilde{\kappa})g_V^\tau \cos\Theta$ which give an experiment some sensitivity to imaginary weak dipole moments in the absence of electron beam polarization.

Instead of measuring $T_x^{\pm}$ and $T_y^{\pm}$ we fit directly for the real and imaginary parts of a_τ^w and d_τ^w using an unbinned maximum likelihood fit. The probability density function (PDF) of the likelihood fit is based on the multi-differential cross-section for $\tau^+\tau^-$ production and decay. The experimental input to the likelihood fit consists of the electron beam polarization, the laboratory frame four-vectors of the e^-, μ^-, π^+ or ρ^+, and the ρ^+ rest frame four-vectors of the π^+ and π^0 produced in ρ^+ decay.

The operation of the SLAC Linear Collider (SLC) with a polarized electron beam has been described previously [6]. During the 1993-1998 running period, SLD recorded $\sim$550,000 hadronic Z decays at a mean center of mass energy of 91.24 GeV with an average longitudinal electron beam polarization of 73.3$\pm$0.8%. Charged particle tracking is provided by the Central Drift Chamber (CDC) and a CCD-based pixel vertex detector (VXD) within a uniform axial magnetic field of 0.6T. The Liquid Argon Calorimeter (LAC) is used for triggering, event selection, tau decay identification, and energy measurement of tau decay products. Muons are identified with the Warm Iron Calorimeter (WIC). A more detailed description of the above detector components can be found in [7].

Our Monte Carlo simulation of $Z \to \tau^+\tau^-$ uses the KORALZ [8] and KORALB [9] generators. The KORALZ generator contains electroweak radiative corrections but does not simulate transverse spin correlations. When run on the Z resonance the KORALB generator does not contain radiative corrections to $\tau^+\tau^-$ production but does contain transverse spin correlations. The MC detector simulation is based on GEANT 3.21 [10].

The selection of tau-pair events begins with the requirement that the number of quality charged tracks, N_{qual}, be in the range $2 \leq N_{qual} \leq 4$, where a quality charged track is one with $|\cos\theta| < 0.80$, two-dimensional transverse impact parameter < 2.0 mm, and three-dimensional impact parameter < 5.0 mm. Here θ is the angle a charged track makes with the beam axis and the term transverse is defined with respect to the beam axis. If $N_{qual} = 2$ then the acollinearity angle formed by the two tracks must be $> 0.3^\circ$ in order to reject Bhabhas and muon-pair events.

Charged tracks and unassociated LAC clusters [11] which satisfy $|\cos\theta| < 0.80$ are divided into two hemispheres defined by the plane perpendicular to the thrust axis. At least one of the two hemispheres must contain exactly one quality charged track. The event thrust axis is required to be within $|\cos\theta_{thrust}| < 0.60$. The four-vectors of the charged tracks and unassociated neutral clusters in each hemisphere are summed together to form the two hemisphere four-vectors. The acollinearity angle formed by the two hemispheres must be $< 18^\circ$ in order to reject two-photon events and events with hard initial state radiation.

We require that every event contain at least one hemisphere that is identified as an e^-, μ^-, π^+, or ρ^+. An identified hemisphere must have one and only one primary charged track. The primary charged track must be a quality charged track. In order to ensure that secondary charged tracks are consistent with photon conversion, as well as to help reject hemispheres that are not consistent with tau decays to e^-, μ^-, π^+, or ρ^+ , we require that an identified hemisphere satisfy the condition $\chi^2_{P\gamma} < 6$. Here

$$\chi^2_{P\gamma} \equiv \frac{M^2_{chg}}{\sigma^2_{chg}} + \frac{M^2_{e\gamma}}{\sigma^2_{e\gamma}} + \frac{(E_{had}/E_P)^2}{\sigma^2_{had}} \quad , \tag{4}$$

where M_{chg} is the invariant mass of the vector sum of any secondary charged tracks, $M_{e\gamma}$ is the invariant mass of the vector sum of any secondary charged tracks and the electromagnetic layer components of any unassociated LAC clusters, E_{had} is the sum of the energies of the hadronic layer components of both associated and unassociated LAC clusters, and E_P is the CDC momentum of the primary charged track.

The parameters σ^2_{chg}, $\sigma^2_{e\gamma}$ and σ^2_{had} in Eq.(4) are the variances of the distributions for M_{chg}, $M_{e\gamma}$ and E_{had}/E_P, respectively, for tau decays to e^-, μ^-, π^+, and ρ^+. The first term in Eq.(4) ensures that secondary charged tracks all come from a single photon, the second term ensures that any direct neutral electromagnetic energy in the hemisphere is due either to a single photon or to a π^0, and the third term is used to reject decays such as $\tau^- \to \pi^+ \bar{K}^0 \nu_\tau$.

The two π^0's in the decay $a_1^+ \to \pi^+\pi^0\pi^0$ often coalesce into a single LAC cluster, making it difficult to distinguish ρ^+ and a_1^+ decays. To ameliorate this situation we use the cluster width in $\zeta \equiv \cos\theta$ and the azimuthal angle about the beam axis, ϕ, to impart a mass to a single LAC cluster.

Assume that a LAC cluster is formed by N_{cl} photons and let E_{cl} be the cluster energy. The momentum of the cluster, $\mathbf{P}_{cl}$, is then

$$\mathbf{P}_{cl} = E_{cl}\boldsymbol{\beta} \ , \quad \boldsymbol{\beta} = \frac{1}{N_{cl}} \sum_i \hat{\mathbf{n}}_i \ \ , \tag{5}$$

where $\hat{\mathbf{n}}_i$ is the direction of photon i. The magnitude of the cluster velocity is

$$|\boldsymbol{\beta}| = \frac{1}{N_{cl}} \sum_i \hat{\mathbf{n}}_i \cdot \hat{\mathbf{n}}_0 = 1 - \left[\frac{\sin^2\theta}{2} \left(\frac{\sigma^2_\zeta}{\sin^4\theta} + \sigma^2_\phi \right) - \sigma^2_0 \right] \tag{6}$$

where $\hat{\mathbf{n}}_0$ is the direction of the cluster, σ_ζ and σ_ϕ are the LAC cluster widths in ζ and ϕ respectively, and the quantity σ_0 is a correction factor used to account for the nonzero cluster widths of single photons. The effect of this formalism on the hemisphere neutral mass distribution is shown in Fig. 1.

Using the above refinement to the definition of LAC cluster four-vectors we calculate the hemisphere energy and mass, E_{hemi} and M_{hemi}, by summing together the four-vectors of

the primary charged track and the electromagnetic layer components of those unassociated LAC clusters which are within 37° of the primary charged track. The energy and mass obtained by summing together only the unassociated cluster four-vectors are denoted by E_{neu} and M_{neu}, respectively.

Electrons are identified in the standard way by the energy and shower profile of the LAC cluster associated with the charged track [12]. Muons are identified by their penetration into the WIC [13]. Electrons and muons furthermore must have their hemisphere energy in the range $5 < E_{hemi} < 36$ GeV in order to suppress two-photon, Bhabha, and muon pair background, and their hemisphere mass must satisfy $M_{hemi} < 0.26$ GeV for hemispheres with $E_{neu} > 0.5$ GeV in order to reject events with hard final state radiation.

A hemisphere is identified as a single π^+ decay if it is not identified as an electron or muon, if $M_{hemi} < 0.26$ GeV for hemispheres with $E_{neu} > 0.5$ GeV, if $E_{had}/E_P < 1.7$, and if $5 < E_{hemi} < 44$ GeV. A hemisphere is identified as a ρ^+ if it is not identified as an electron, muon, or π^+, and if it satisfies the conditions $E_{had}/E_P < 2.5$, $M_{neu} < 0.48$ GeV, $0.35 < M_{hemi} < 1.20$ GeV, and $5 < E_{hemi} < 44$ GeV.

Applying the above criteria to the 1993–1998 SLD data sample we select a total of 6736 tau pairs, with 2016 electron, 2577 muon, 1847 pion, 3799 rho, and 3233 unidentified hemispheres, where unidentified means that the hemisphere was not identified as an e^-, μ^-, π^+, or ρ^+ .

The tau selection efficiency and purity as calculated by Monte Carlo are shown in Table 1. The electron and muon samples are very clean. The single pion sample receives roughly equal background from misidentified electron, muons and rho's. Most of the contamination of the rho sample comes from misidentified $a_1 \to \pi^+\pi^0\pi^0$ decays. The non–τ background from two-photon, Bhabha's, muon pairs, and hadronic events is estimated to be 0.38%, 0.87%, 0.2%, and 0.01% respectively.

As a check on the Monte Carlo detection efficiency calculation the momentum distributions for hemispheres identified as e^-, μ^-, π^+, and ρ^+ are shown in Fig. 2 for data and

Monte Carlo. Correctly and incorrectly identified decays are summed together in the Monte Carlo curves. A single normalization factor is used to scale the Monte Carlo to the data so that these plots also serve to check the absolute normalization of the efficiency calculations for different decay modes.

The identification and misidentification efficiencies for tau decay modes as a function of kinematic variables are incorporated into the PDF of the likelihood fit. Detector resolution, radiative corrections, and non–τ background are not included in the fit, however. The PDF is then a sum of lowest-order multi-differential cross-section expressions for $\tau^+\tau^-$ production and decay modulated by identification or misidentification efficiency functions.

The multi-differential cross-section is calculated using helicity amplitude expressions for $\tau^+\tau^-$ production [14] and τ decay [15, 16]. In order to calculate the multi-differential cross-section the τ^- direction must be specified. No attempt is made to measure the tau direction, however. For events with two semi-hadronic decays there is a discrete two-fold ambiguity in the tau direction which is summed over in the likelihood fit. For events with a leptonic decay or with an unidentified hemisphere the ambiguity is continuous and an integration is performed over possible tau directions.

Applying our likelihood fit to the data we obtain initial estimates of $Re(a_\tau^w) = (1.16 \pm 0.99) \times 10^{-3}$, $Im(a_\tau^w) = (-0.27 \pm 0.62) \times 10^{-3}$, $Re(d_\tau^w) = (\ 0.18 \pm 0.61) \times 10^{-17} e \cdot cm$, and $Im(d_\tau^w) = (-0.14 \pm 0.35) \times 10^{-17} e \cdot cm$, where the errors are statistical. Our final estimates are obtained by making corrections to these values in order to account for effects not included in the PDF of the likelihood fit.

The absence of a detector resolution function, QED radiative corrections and non-τ background in the PDF produces shifts in the fitted values of the anomalous moments with respect to their true values. The KORALZ Monte Carlo is used to calculate the shifts due to the combined effects of detector resolution and QED radiative corrections, while the shifts due to detector resolution alone are calculated using the KORALB Monte Carlo. The shifts

due to non-τ background are calculated by adding a Monte Carlo sample of the background to the KORALZ Monte Carlo sample. The results are summarized in Table 2.

Our systematic error is dominated by the uncertainties in the shifts in Table 2. For the detector systematic errors we conservatively use the entire detector effects shifts from Table 2, taking into account the KORALB Monte Carlo statistical errors. Specifically, we assume that the sum in quadrature of the detector systematic error and the KORALB statistical error is equal to the detector effects shift. If the detector systematic error extracted under this assumption is less than the KORALB statistical error then we set the detector systematic error equal to the KORALB statistical error.

The systematic errors in the calculation of the shifts due to QED radiative corrections and non-τ background are estimated using the Monte Carlo statistical errors for the KORALZ and non-τ background Monte Carlo samples. The resulting systematic errors are summarized in Table 3.

Applying the corrections of Table 2 to our initial estimates of a_τ^w and d_τ^w we obtain our final results:

$$\begin{aligned} Re(a_\tau^w) &= (0.26 \pm 0.99 \pm 0.75) \times 10^{-3} \\ Im(a_\tau^w) &= (-0.02 \pm 0.62 \pm 0.24) \times 10^{-3} \\ Re(d_\tau^w) &= (\ 0.18 \pm 0.61 \pm 0.28) \times 10^{-17} e \cdot cm \\ Im(d_\tau^w) &= (-0.26 \pm 0.35 \pm 0.13) \times 10^{-17} e \cdot cm \end{aligned} \tag{7}$$

where the first error is statistical and the second error is systematic. The results are consistent with the standard model expectation of ≈ 0. Our 95% confidence level limits are $|Re(a_\tau^w)| < 2.48 \times 10^{-3}$, $|Im(a_\tau^w)| < 1.30 \times 10^{-3}$, $|Re(d_\tau^w)| < 1.36 \times 10^{-17} e \cdot cm$, and $|Im(d_\tau^w)| < 0.87 \times 10^{-17} e \cdot cm$. With the exception of $Re(d_\tau^w)$, all of our limits are improvements over previously published limits for a_τ^w [17] and d_τ^w [18, 19].

We would like to thank the personnel of the SLAC accelerator department and the technical staffs of our collaborating institutions for their outstanding efforts on our behalf.

We would also like to thank Michael Peskin and Tom Rizzo for theoretical guidance. This work was supported by the U.S. Department of Energy and National Science Foundation, the UK Particle Physics and Astronomy Research Council, the Istituto Nazionale di Fisica Nucleare of Italy, and the Japan-US Cooperative Research Project on High Energy Physics.

References

[1] J. Bernabéu, G.A. González-Sprinberg, M. Tung, J. Vidal, *Nucl. Phys.* **B436**, 474 (1995).

[2] M.J. Booth, University of Chicago Report No. EFI-93-01 (1993).

[3] W. Bernreuther, U. Löw, J.P. Ma, O. Nachtmann, *Z. Phys.* **C43**, 117 (1989).

[4] T.G. Rizzo, *Phys. Rev.* **D51**, 3811 (1995).

[5] E.C. Torrence, Ph.D thesis, Massachusetts Institute of Technology, 1997, SLAC-REPORT-509.

[6] K. Abe *et al.*, *Phys. Rev. Lett.* **78**, 2075 (1997).

[7] K. Abe *et al.*, *Phys. Rev.* **D53**, 1023 (1996).

[8] S. Jadach, B.F.L. Ward, and Z. Wąs, *Comp. Phys. Comm.* **66**, 276 (1991).

[9] S. Jadach and Z. Wąs, *Comp. Phys. Comm.* **36**, 191 (1985); *Comp. Phys. Comm.* **64**, 267 (1991); *Comp. Phys. Comm.* **85**, 453 (1995).

[10] R. Brun *et al.*, Report No. CERN-DD-78-2-REV (1978).

[11] Saul Gonzalez Martirena, Ph.D thesis, Stanford University, 1994, SLAC-REPORT-439.

[12] K. Abe *et al.*, Report No. SLAC-PUB-7798 (1999).

[13] David C. Williams, Ph.D thesis, Stanford University, 1994, SLAC-REPORT-445.

[14] G. Kane, G.A. Ladinsky, and C.-P. Yuan, *Phys. Rev.* **D45**, 124 (1992).

[15] K. Hagiwara and D. Zeppenfeld, *Nucl. Phys.* **B274**, 1 (1986).

[16] S. Jadach, J.H. Kühn, and Z. Wąs, *Comp. Phys. Comm.* **64**, 275 (1991).

[17] M. Acciarri *et al.*, *Phys. Lett.* **B426**, 207 (1998).

[18] D. Buskulic *et al.*, *Phys. Lett.* **B346**, 371 (1995).

[19] K. Ackerstaff *et al.*, *Z. Phys.* **C74**, 403 (1997).

[†]**The SLD Collaboration**

Kenji Abe,[21] Koya Abe,[33] T. Abe,[29] I. Adam,[29] T. Akagi,[29] H. Akimoto,[29] N.J. Allen,[5] W.W. Ash,[29,*] D. Aston,[29] K.G. Baird,[17] C. Baltay,[40] H.R. Band,[39] M.B. Barakat,[16] O. Bardon,[19] T.L. Barklow,[29] G.L. Bashindzhagyan,[20] J.M. Bauer,[18] G. Bellodi,[23] A.C. Benvenuti,[3] G.M. Bilei,[25] D. Bisello,[24] G. Blaylock,[17] J.R. Bogart,[29] G.R. Bower,[29] J.E. Brau,[22] M. Breidenbach,[29] W.M. Bugg,[32] D. Burke,[29] T.H. Burnett,[38] P.N. Burrows,[23] R.M. Byrne,[19] A. Calcaterra,[12] D. Calloway,[29] B. Camanzi,[11] M. Carpinelli,[26] R. Cassell,[29] R. Castaldi,[26] A. Castro,[24] M. Cavalli-Sforza,[35] A. Chou,[29] E. Church,[38] H.O. Cohn,[32] J.A. Coller,[6] M.R. Convery,[29] V. Cook,[38] R.F. Cowan,[19] D.G. Coyne,[35] G. Crawford,[29] C.J.S. Damerell,[27] M.N. Danielson,[8] M. Daoudi,[29] N. de Groot,[4] R. Dell'Orso,[25] P.J. Dervan,[5] R. de Sangro,[12] M. Dima,[10] D.N. Dong,[19] M. Doser,[29] R. Dubois,[29] B.I. Eisenstein,[13] I.Erofeeva,[20] V. Eschenburg,[18] E. Etzion,[39] S. Fahey,[8] D. Falciai,[12] C. Fan,[8] J.P. Fernandez,[35] M.J. Fero,[19] K. Flood,[17] R. Frey,[22] J. Gifford,[36] T. Gillman,[27] G. Gladding,[13] S. Gonzalez,[19] E.R. Goodman,[8] E.L. Hart,[32] J.L. Harton,[10] K. Hasuko,[33] S.J. Hedges,[6] S.S. Hertzbach,[17] M.D. Hildreth,[29] J. Huber,[22] M.E. Huffer,[29] E.W. Hughes,[29] X. Huynh,[29] H. Hwang,[22] M. Iwasaki,[22] D.J. Jackson,[27] P. Jacques,[28] J.A. Jaros,[29] Z.Y. Jiang,[29] A.S. Johnson,[29] J.R. Johnson,[39] R.A. Johnson,[7] T. Junk,[29] R. Kajikawa,[21] M. Kalelkar,[28] Y. Kamyshkov,[32] H.J. Kang,[28] I. Karliner,[13] H. Kawahara,[29] Y.D. Kim,[30] M.E. King,[29] R. King,[29] R.R. Kofler,[17] N.M. Krishna,[8] R.S. Kroeger,[18] M. Langston,[22] A. Lath,[19] D.W.G. Leith,[29] V. Lia,[19] C.Lin,[17] M.X. Liu,[40] X. Liu,[35] M. Loreti,[24] A. Lu,[34] H.L. Lynch,[29] J. Ma,[38] M. Mahjouri,[19] G. Mancinelli,[28] S. Manly,[40] G. Mantovani,[25] T.W. Markiewicz,[29] T. Maruyama,[29] H. Masuda,[29] E. Mazzucato,[11] A.K. McKemey,[5] B.T. Meadows,[7] G. Menegatti,[11] R. Messner,[29] P.M. Mockett,[38] K.C. Moffeit,[29] T.B. Moore,[40] M.Morii,[29] D. Muller,[29] V. Murzin,[20] T. Nagamine,[33] S. Narita,[33] U. Nauenberg,[8] H. Neal,[29] M. Nussbaum,[7,*] N. Oishi,[21] D. Onoprienko,[32] L.S. Osborne,[19] R.S. Panvini,[37] C.H. Park,[31] T.J. Pavel,[29] I. Peruzzi,[12] M. Piccolo,[12] L. Piemontese,[11] K.T. Pitts,[22] R.J. Plano,[28] R. Prepost,[39] C.Y. Prescott,[29] G.D. Punkar,[29] J. Quigley,[19] B.N. Ratcliff,[29] T.W. Reeves,[37] J. Reidy,[18] P.L. Reinertsen,[35] P.E. Rensing,[29] L.S. Rochester,[29] P.C. Rowson,[9] J.J. Russell,[29] O.H. Saxton,[29] T. Schalk,[35] R.H. Schindler,[29] B.A. Schumm,[35] J. Schwiening,[29] S. Sen,[40] V.V. Serbo,[29] M.H. Shaevitz,[9] J.T. Shank,[6] G. Shapiro,[15] D.J. Sherden,[29] K.D. Shmakov,[32] C. Simopoulos,[29] N.B. Sinev,[22] S.R. Smith,[29] M.B. Smy,[10] J.A. Snyder,[40] H. Staengle,[10] A. Stahl,[29] P. Stamer,[28] H. Steiner,[15] R. Steiner,[1] M.G. Strauss,[17] D. Su,[29] F. Suekane,[33]

A. Sugiyama,[21] S. Suzuki,[21] M. Swartz,[14] A. Szumilo,[38] T. Takahashi,[29]
F.E. Taylor,[19] J. Thom,[29] E. Torrence,[19] N.K. Toumbas,[29] T. Usher,[29]
C. Vannini,[26] J. Va'vra,[29] E. Vella,[29] J.P. Venuti,[37] R. Verdier,[19] P.G. Verdini,[26]
D.L. Wagner,[8] S.R. Wagner,[29] A.P. Waite,[29] S. Walston,[22] S.J. Watts,[5]
A.W. Weidemann,[32] E. R. Weiss,[38] J.S. Whitaker,[6] S.L. White,[32] F.J. Wickens,[27]
B. Williams,[8] D.C. Williams,[19] S.H. Williams,[29] S. Willocq,[17] R.J. Wilson,[10]
W.J. Wisniewski,[29] J. L. Wittlin,[17] M. Woods,[29] G.B. Word,[37] T.R. Wright,[39]
J. Wyss,[24] R.K. Yamamoto,[19] J.M. Yamartino,[19] X. Yang,[22] J. Yashima,[33]
S.J. Yellin,[34] C.C. Young,[29] H. Yuta,[2] G. Zapalac,[39] R.W. Zdarko,[29] J. Zhou.[22]

(The SLD Collaboration)

[1] *Adelphi University, Garden City, New York 11530,*
[2] *Aomori University, Aomori , 030 Japan,*
[3] *INFN Sezione di Bologna, I-40126, Bologna, Italy,*
[4] *University of Bristol, Bristol, U.K.,*
[5] *Brunel University, Uxbridge, Middlesex, UB8 3PH United Kingdom,*
[6] *Boston University, Boston, Massachusetts 02215,*
[7] *University of Cincinnati, Cincinnati, Ohio 45221,*
[8] *University of Colorado, Boulder, Colorado 80309,*
[9] *Columbia University, New York, New York 10533,*
[10] *Colorado State University, Ft. Collins, Colorado 80523,*
[11] *INFN Sezione di Ferrara and Universita di Ferrara, I-44100 Ferrara, Italy,*
[12] *INFN Lab. Nazionali di Frascati, I-00044 Frascati, Italy,*
[13] *University of Illinois, Urbana, Illinois 61801,*
[14] *Johns Hopkins University, Baltimore, Maryland 21218-2686,*
[15] *Lawrence Berkeley Laboratory, University of California, Berkeley, California 94720,*
[16] *Louisiana Technical University, Ruston,Louisiana 71272,*
[17] *University of Massachusetts, Amherst, Massachusetts 01003,*
[18] *University of Mississippi, University, Mississippi 38677,*
[19] *Massachusetts Institute of Technology, Cambridge, Massachusetts 02139,*
[20] *Institute of Nuclear Physics, Moscow State University, 119899, Moscow Russia,*
[21] *Nagoya University, Chikusa-ku, Nagoya, 464 Japan,*
[22] *University of Oregon, Eugene, Oregon 97403,*
[23] *Oxford University, Oxford, OX1 3RH, United Kingdom,*
[24] *INFN Sezione di Padova and Universita di Padova I-35100, Padova, Italy,*
[25] *INFN Sezione di Perugia and Universita di Perugia, I-06100 Perugia, Italy,*
[26] *INFN Sezione di Pisa and Universita di Pisa, I-56010 Pisa, Italy,*
[27] *Rutherford Appleton Laboratory, Chilton, Didcot, Oxon OX11 0QX United Kingdom,*
[28] *Rutgers University, Piscataway, New Jersey 08855,*
[29] *Stanford Linear Accelerator Center, Stanford University, Stanford, California 94309,*
[30] *Sogang University, Seoul, Korea,*
[31] *Soongsil University, Seoul, Korea 156-743,*
[32] *University of Tennessee, Knoxville, Tennessee 37996,*
[33] *Tohoku University, Sendai 980, Japan,*

[34] *University of California at Santa Barbara, Santa Barbara, California 93106,*
[35] *University of California at Santa Cruz, Santa Cruz, California 95064,*
[36] *University of Victoria, Victoria, British Columbia, Canada V8W 3P6,*
[37] *Vanderbilt University, Nashville,Tennessee 37235,*
[38] *University of Washington, Seattle, Washington 98105,*
[39] *University of Wisconsin, Madison,Wisconsin 53706,*
[40] *Yale University, New Haven, Connecticut 06511.*

* Deceased.

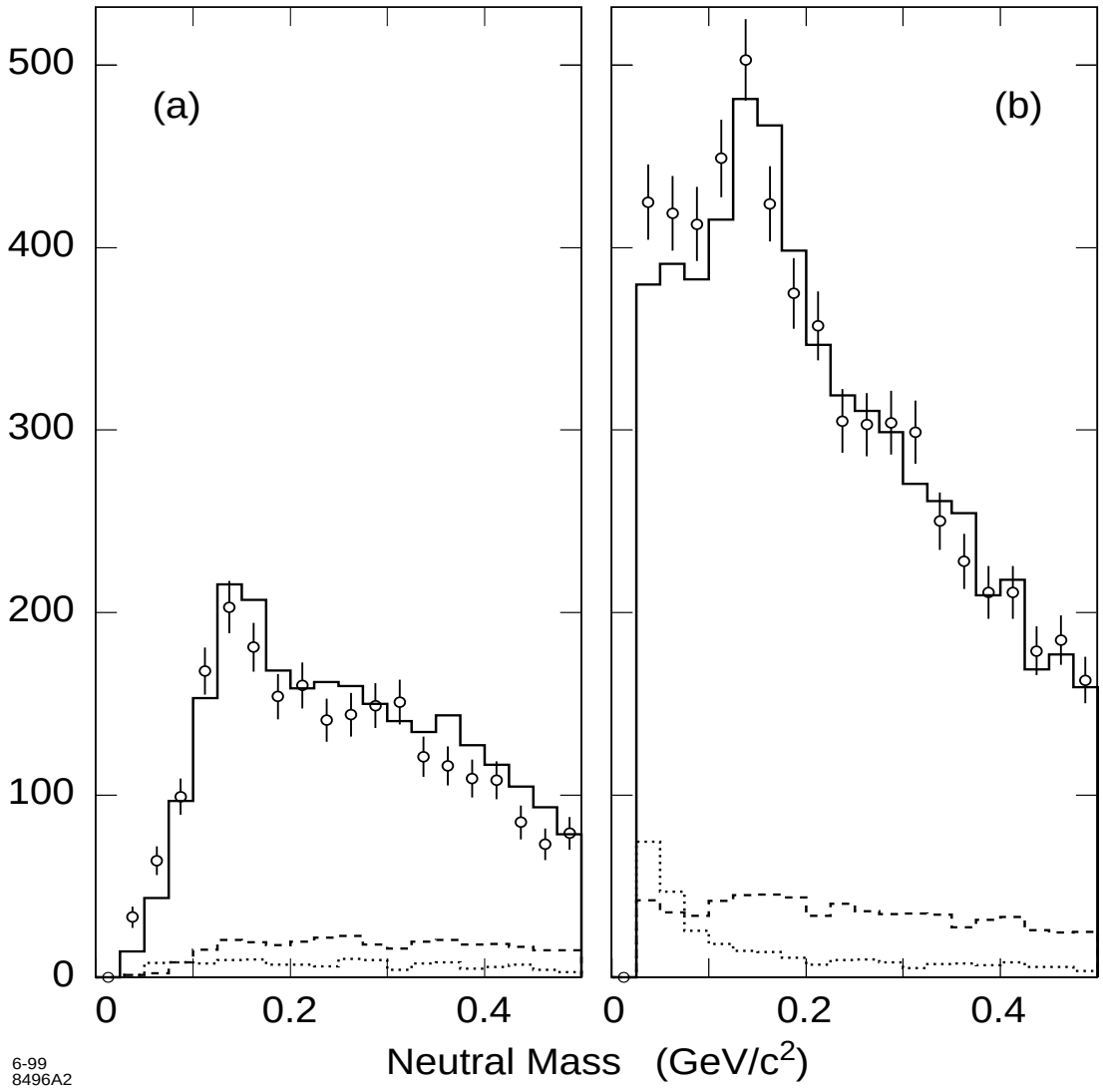

Figure 1: Hemisphere neutral mass M_{neu} for (a) LAC cluster $\beta = 1$ and (b) LAC cluster β as given by Eq. 6. Hemispheres with $M_{neu} = 0$ have been excluded. The open circles are data and the solid, dashed, and dotted lines are Monte Carlo simulations for all tau decays, a_1^+ decays, and π^+ decays, respectively.

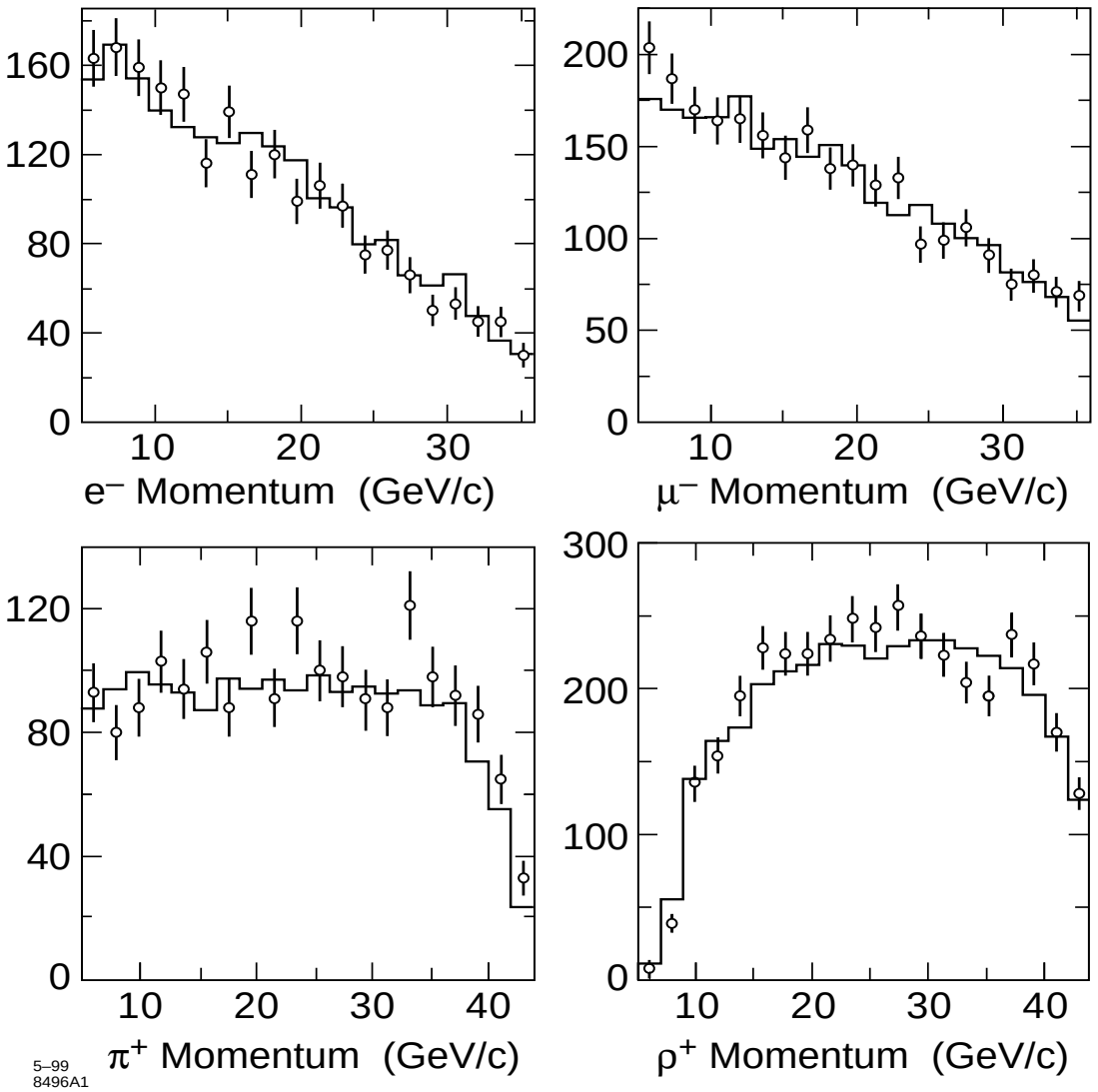

Figure 2: Momentum distributions for e^-, μ^-, π^+, and ρ^+ candidates. The open circles are data and the solid lines are Monte Carlo simulation.

Table 1: τ decay identification efficiency and purity

Mode	Efficiency	Purity	Number of Events
$e^-\bar{\nu}_e\nu_\tau$	0.74	0.96	2016
$\mu^-\bar{\nu}_\mu\nu_\tau$	0.93	0.96	2577
$\pi^+\nu_\tau$	0.76	0.74	1847
$\rho^+\nu_\tau$	0.70	0.83	3799

Table 2: Shifts in fitted values of a_τ^w and d_τ^w.

Source	$Re(a_\tau^w)$ (10^{-3})	$Im(a_\tau^w)$ (10^{-3})	$Re(d_\tau^w)$ $(10^{-17} e \cdot cm)$	$Im(d_\tau^w)$ $(10^{-17} e \cdot cm)$
detector effects	-0.637	-0.064	-0.023	0.052
QED rad. corr.	1.221	-0.234	0.031	0.075
Non-τ events	0.321	0.046	-0.005	-0.011
Total	0.905	-0.252	0.003	0.116

Table 3: Systematic errors in a_τ^w and d_τ^w.

Source	$Re(a_\tau^w)$ (10^{-3})	$Im(a_\tau^w)$ (10^{-3})	$Re(d_\tau^w)$ $(10^{-17} e \cdot cm)$	$Im(d_\tau^w)$ $(10^{-17} e \cdot cm)$
detector effects	0.585	0.120	0.134	0.067
QED rad. corr.	0.421	0.185	0.224	0.099
Non-τ events	0.189	0.087	0.108	0.048
Total	0.745	0.237	0.282	0.129